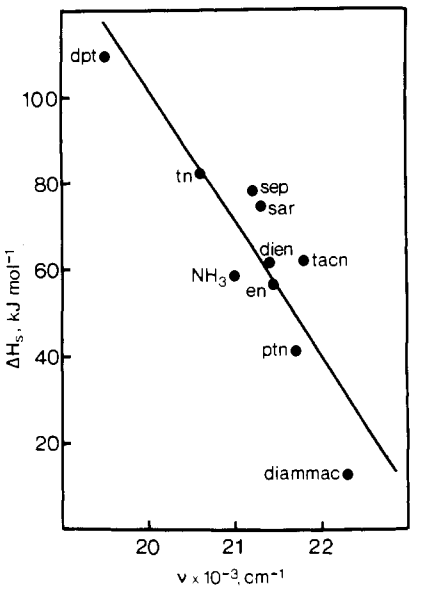

Figure 4. Plot of the steric relaxation energy against the frequency of the low-energy d–d electronic transition for the complexes listed in Table I. The line of best fit is shown.

Co–N bond length of 2.05–2.10 Å in the excited state. It appears from the present calculations that the frequency of spectral transitions is correlated with strain relaxation. This is observable qualitatively; highly strained complexes such as $[Co(dpt)_2]^{3+}$ are red, while less strained complexes or those with compressed Co–N bonds are yellow. The observed correlation between reduction potential and frequency of the d–d transition (Figure 3) is probably due to both processes being influenced by the steric relaxation that occurs on extension of the Co–N bond.

A variation in ligand field strength with hole size for (tetraaza macrocycle)cobalt(III) complexes has been reported by Busch et al.[10] who suggested that the higher ligand field observed for smaller macrocycles resulted from compression of the metal–ligand bonds. This accords with the present analysis, since extension of a compressed Co–N bond would require more energy. Thom et al.[35] put forward the alternative explanation that the ligand field was at its maximum when the ligands best fit the metal, since this gave maximum orbital overlap. We do not rule this out as a plausible explanation for the variation in ligand field strength, since there is an obvious correlation between Co(III)–N bond length and the frequency of the low-energy d–d transition for the complexes considered here (Tables I and II). If this explanation is correct, then the correlation between reduction potential and the frequency of the low-energy d–d transition is a consequence of the coincidental correlation between the Co(III)–N bond length and the steric relaxation energy.

(35) Thom, V. J.; Boeyens, J. C. A.; McDougall, G. J.; Hancock, R. D. *J. Am. Chem. Soc.* **1984**, *106*, 3198–207.

Conclusions

It is clear from the present study that relaxation of strain which occurs on extension of the Co–N bond length concomitant with Co(III)/Co(II) reduction contributes significantly to the thermodynamics of the reduction process. Indeed, for the complexes considered, it is the major cause for the observed differences in reduction potential. Therefore, when differences in redox potentials are analyzed for those cases in which a significant change in the metal–ligand bond length occurs, the effects of steric strain must be taken into account. We have also shown that the molecular mechanics method can be used to calculate and so delineate the steric relaxation contribution to reduction potentials in order that other contributions can be more easily investigated. In so doing, we have demonstrated a possible dependence of the reduction potential on the Lewis basicity of the ligand. This study also shows how steric aspects of ligand design might be used to produce desired redox properties.

A correlation between steric relaxation resulting from extension of the Co–N bonds and the frequency of the low-energy d–d transition has also been established, indicating a possible steric contribution to ligand field strength. This suggests that this electronic transition is also accompanied by a change in the metal–ligand bond length and may explain the correlation that has been observed between reduction potential and the frequency of the d–d transition.

Acknowledgment. We wish to thank Dr P. A. Lay for critical comment and helpful discussion.

Registry No. $[Co(NH_3)_6]^{3+}$, 14695-95-5; $[Co(NH_3)_3]^{2+}$, 15365-75-0; $[Co(en)_3]^{3+}$, 14878-41-2; $[Co(en)_3]^{2+}$, 23523-25-3; $[Co(tn)_3]^{3+}$, 16786-53-1; $[Co(tn)_3]^{2+}$, 46469-74-3; $[Co(dien)_2]^{3+}$, 18703-28-1; $[Co(dien)_2]^{2+}$, 23624-01-3; $[Co(dpt)_2]^{3+}$, 86709-83-3; $[Co(dpt)_2]^{2+}$, 113376-50-4; $[Co(ptn)_2]^{3+}$, 113430-55-0; $[Co(ptn)_2]^{2+}$, 113376-54-8; $[Co(tacn)_2]^{3+}$, 89637-25-2; $[Co(tacn)_2]^{2+}$, 91760-59-7; [Co(diammac)]$^{3+}$, 114595-74-3; [Co(diammac)]$^{2+}$, 114595-75-4; [Co(sep)]$^{3+}$, 72496-77-6; [Co(sep)]$^{2+}$, 63218-22-4; [Co(sar)]$^{3+}$, 85663-77-0; [Co(sar)]$^{2+}$, 71935-80-3.

Contribution No. 7690 from the Arthur Amos Noyes Laboratory, California Institute of Technology, Pasadena, California 91125

Electronic Spectra of $Ru_2(carboxylate)_4^+$ Complexes. Higher Energy Electronic Excited States

Vincent M. Miskowski* and Harry B. Gray*

Received December 4, 1987

Solution (CH_3CN, CH_2Cl_2, CH_3OH, poly(methyl methacrylate)) electronic absorption data are reported for $[Ru_2(butyrate)_4X_n]^{(1-n)+}$ (n = 0, 1, 2; X = Cl, Br, I). Single-crystal visible absorption data are reported for $Ru_2(propionate)_4Cl$, $Ru_2(acetate)_4Cl$, $Ru_2(butyrate)_4Br$, and two crystal forms of $Ru_2(butyrate)_4Cl$. The only visible absorption band that develops vibronic structure at low temperature is an ~570-nm $\perp$ c-polarized feature of the $I\bar{4}2d$ polymorph of $Ru_2(butyrate)_4Cl$; the long progression in $\Delta\nu \approx 330$ cm^{-1} is attributed to the excited-state ν(Ru–O). The transition is assigned to $\delta^*(Ru_2) \rightarrow \sigma^*$(Ru–O), intensified in a crystal site of low symmetry. A molecular x,y-polarized transition at ~570 nm (ϵ = 150–200) in all of the compounds is assigned to $\pi^*(Ru_2) \rightarrow \sigma^*$(Ru–O). Assignments of π(Ru–O,Ru_2) $\rightarrow \sigma^*$(Ru–O) and $\delta(Ru_2) \rightarrow \pi^*(Ru_2)$ are suggested for an x,y-polarized system at ~450 nm (ϵ = 70–135) and an extremely weak ($\epsilon \approx 20$) band at ~630 nm, while an intense band at ~460 nm ($\epsilon \approx$ 1000) is assigned to π(Ru–O,Ru_2) $\rightarrow \pi^*(Ru_2)$. An intense (ϵ = 4000–10 000) axial halide sensitive band in the near-UV region is assigned to an axial ligand-to-metal charge-transfer transition, most likely $\pi(X) \rightarrow \pi^*(Ru_2)$.

The diruthenium(II,III) carboxylates, $Ru_2(O_2CR)_4^+$, possess a remarkable spin-quartet ground state.[1,2] This ground state was eventually explained by Norman and co-workers[3] according to the pattern of metal–metal bonding and antibonding orbitals that

0020-1669/88/1327-2501$01.50/0

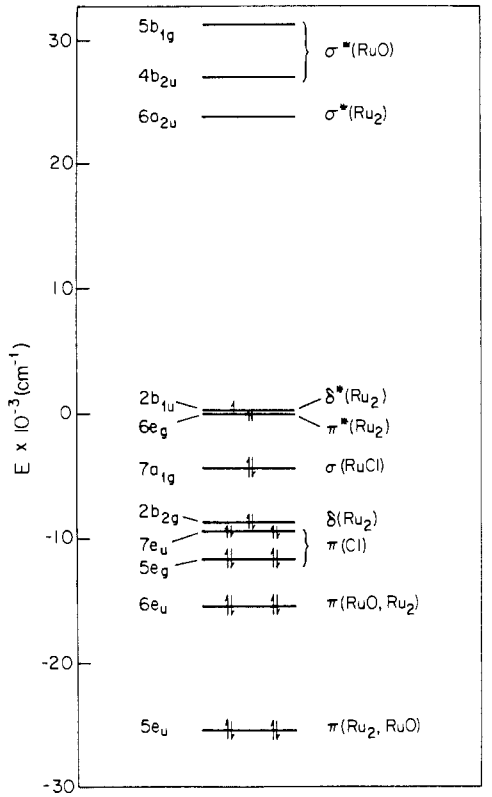

Figure 1. Partial energy level diagram for $[Ru_2(O_2CH)_4Cl_2]^-$ from ref 3c. The energy of $6e_g$ has been set equal to zero for convenience.

emerged from their SCF-Xα calculations. The calculated levels[3c] for $[Ru_2(O_2CH)_4Cl_2]^-$ are shown in Figure 1. The π^* and δ^* orbitals turn out to be nearly degenerate, and a high-spin (quartet) ground state results.

The pattern of calculated energy levels[3] is very similar for carboxylato-bridged metal dimers possessing metal–metal bond orders ranging from 1 (δ^* and π^* filled) to 4 (δ^* and π^* empty). The diruthenium(II,III) carboxylates thus would be predicted to show low-energy electronic transitions, including those typical of both bond order extremes. The bond order 1 system shows[4,5] low-energy transitions involving excitations from π^* and δ^* orbitals to $\sigma^*(M_2)$ and $\sigma^*(M-O)$ orbitals, while the bond order 4 species exhibits[6,7] metal–metal transitions such as $\delta \rightarrow \delta^*$.

In a recent paper[8] we presented a detailed study of the near-infrared electronic absorption spectra of the diruthenium(II,III) carboxylates, concentrating on polarized single-crystal spectra. We identified the $\delta \rightarrow \delta^*$ transition, with an electronic origin at $\sim$9000 cm^{-1}, together with several weak spin-forbidden transitions within the $(\pi^*\delta^*)^3$ configuration, including $\pi^* \rightarrow \delta^*$ with an electronic origin at $\sim$6900 cm^{-1}.

We have extended our studies of the electronic absorption spectra of the diruthenium(II,III) carboxylates to the visible and near-ultraviolet regions. In this paper we report both solution and single-crystal spectra in these regions. The new data available have allowed us to make more detailed transition assignments than were made in the earlier study of $Ru_2(O_2CMe)_4Cl$ by Martin et al.[9]

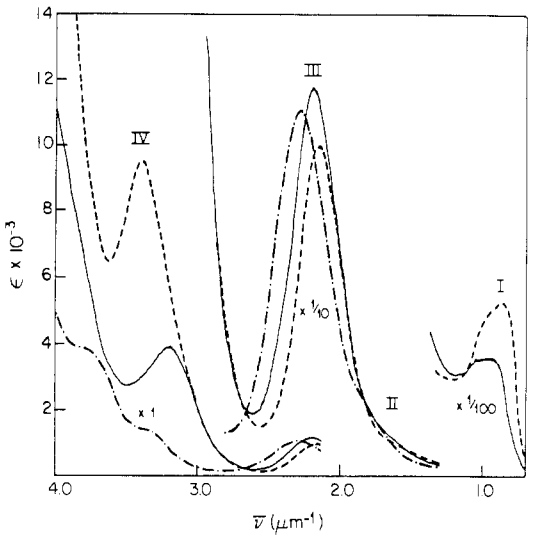

Figure 2. Electronic spectra of $Ru_2(O_2CPr)_4Cl$: (—) in CH_3CN at room temperature; (- - -) in 0.01 M [TEA]Cl solution; (–·–) after precipitation of Cl^- with stoichiometric $AgBF_4$.

Experimental Section

Acetonitrile (Burdick and Jackson) and methylene chloride (MCB) were spectroquality. Commercial [TEA]Cl, [TBA]Br, [TBA]I, and [TBA]ClO_4 were freshly recrystallized from CH_2Cl_2 and vacuum-dried (TEA is tetraethylammonium, and TBA is tetra-*n*-butylammonium). An electronic spectrum of [TBA]I in CH_2Cl_2 showed no I_3^-.

Preparation and crystallization of the ruthenium carboxylate compounds have been described.[8] Single-crystal spectroscopic techniques were similar to those previously employed.[5,6b]

Solution Electronic Spectra

Electronic spectra of $Ru_2(carboxylate)_4^+$ compounds in aqueous and/or methanolic solutions have been reported by a number of groups.[1,10,11] In agreement with them, we find that the spectra are independent of carboxylate alkyl group, and we will present results in this section only for butyrates, which have conveniently high solubilities in polar organic solvents.

While aqueous and methanolic solutions of the $Ru_2(carboxylate)_4Cl$ compounds have conductances consistent with dissociation[1] to $Ru_2(carboxylate)_4(solvent)_2^+$ complexes, we find that solutions in CH_3CN or CH_2Cl_2 are completely nonconducting, as judged by comparisons to solutions of tetraphenylarsonium chloride and to neat solvent. As shown in Figure 2, precipitation of Cl^- with silver ion and addition of excess chloride yield spectral changes consistent with formation of, respectively, bis(solvent) and dichloro complexes. Both types of complexes have been characterized by crystal structures.[12] The neutral species present in neat solution is then presumably the mono(solvent) complex. We note that this finding is not in disagreement with the electrochemical results of Cotton and Pedersen,[2] which indicated considerable chloride dissociation in CH_2Cl_2. A CH_2Cl_2 solution of $Ru_2(O_2CPr)_4Cl$ adjusted to 0.1 M in [TBA]ClO_4, like the solutions those workers investigated, shows a visible absorption maximum shifted to 440 nm and considerably decreased intensity for the 327-nm band of the electrolyte-free solutions; the high electrolyte concentration evidently induces chloride dissociation.

(1) Stephenson, T. A.; Wilkinson, G. *J. Inorg. Nucl. Chem.* **1966**, *28*, 2285.
(2) (a) Cotton, F. A.; Pedersen, E. *Inorg. Chem.* **1975**, *14*, 388. (b) Telser, J.; Drago, R. S. *Inorg. Chem.* **1984**, *23*, 3114.
(3) (a) Norman, J. G., Jr.; Kolari, H. J.; Gray, H. B.; Trogler, W. C. *Inorg. Chem.* **1977**, *16*, 987. (b) Norman, J. G., Jr.; Kolari, H. J. *J. Am. Chem. Soc.* **1978**, *100*, 791. (c) Norman, J. G., Jr.; Renzoni, G. E.; Case, D. A. *J. Am. Chem. Soc.* **1979**, *101*, 5256.
(4) Martin, D. S.; Webb, T. R.; Robbins, G. A.; Fanwick, P. E. *Inorg. Chem.* **1979**, *18*, 475.
(5) (a) Miskowski, V. M.; Schaefer, W. P.; Sadeghi, B.; Santarsiero, B. D.; Gray, H. B. *Inorg. Chem.* **1984**, *23*, 1154. (b) Miskowski, V. M.; Smith, T. P.; Loehr, T. M.; Gray, H. B. *J. Am. Chem. Soc.* **1985**, *107*, 7965.
(6) (a) Trogler, W. C.; Gray, H. B. *Acc. Chem. Res.* **1978**, *11*, 232. (b) Hopkins, M. D.; Miskowski, V. M.; Gray, H. B. *J. Am. Chem. Soc.* **1986**, *108*, 959.
(7) Martin, D. S.; Newman, R. A.; Fanwick, P. E. *Inorg. Chem.* **1979**, *18*, 2511.
(8) Miskowski, V. M.; Loehr, T. M.; Gray, H. B. *Inorg. Chem.* **1987**, *26*, 1098.
(9) Martin, D. S.; Newman, R. A.; Vlasnik, L. M. *Inorg. Chem.* **1980**, *19*, 3404.
(10) Wilson, C. R.; Taube, H. *Inorg. Chem.* **1975**, *14*, 2276.
(11) Mukaida, M.; Nomura, T.; Ishimori, T. *Bull. Chem. Soc. Jpn.* **1972**, *45*, 2143.
(12) (a) Bino, A.; Cotton, F. A.; Felthouse, T. R. *Inorg. Chem.* **1979**, *18*, 2599. (b) Marsh, R. E.; Schomaker, V. *Inorg. Chem.* **1981**, *20*, 299.

Table I. Solution Electronic Spectral Data for $Ru_2(O_2CPr)_4^+$ Complexes[a]

solvent	I	II	III	IV
CH_3OH	990 (25)	~550 (200 sh)	426 (850)	~295 (2500 sh) ~260 (5000 sh)
CH_3CN[b]	*d*	~550 (200 sh)	439 (110)	~300 (1200 sh) ~265 (3800 sh)
CH_3CN	1080 (36)	~610 (120 sh)	458 (1170)	312 (3900)
CH_2Cl_2	*d*	~580 (140 sh)	456 (110)	321 (4200)
CH_3CN[c]	1100 (40)	~620 (150 sh)	469 (1500)	353 (2700)
CH_3CN, 0.01 M [TEA]Cl	1150 (52)	~630 (90 sh)	466 (990)	296 (9300)
CH_3CN, 0.1 M [TBA]Br	1150 (56)	~670 (70 sh)	470 (1130)	343 (7200)
CH_3CN, 0.5 M [TBA]I	1150 (98)	~700 (100 sh)	533 (2120)	421 (5400)

[a] The ruthenium source was $Ru_2(O_2CPr)_4Cl$ except where noted. Each entry is in the form λ_{max} (nm) with ϵ_{max} in parentheses. [b] Chloride precipitated with stoichiometric $AgBF_4$. [c] Compound was $Ru_2(O_2CPr)_4Br$. [d] Not measured.

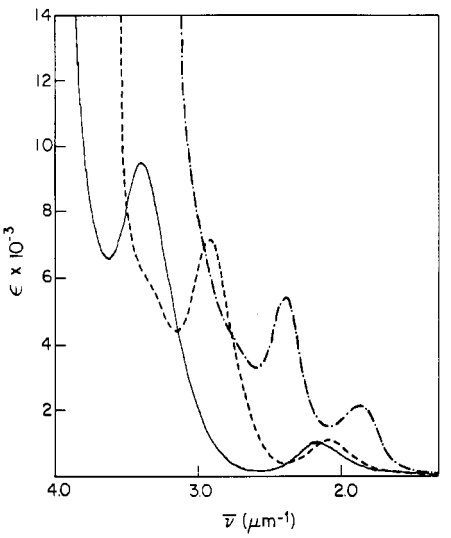

Figure 3. Electronic spectra of $[Ru_2(O_2CPr)_4X_2]^-$ complexes in CH_3CN: (—) X = Cl; (---) X = Br; (-·-) X = I. For X = Cl and Br, the solution was 0.01 M in [TEA]Cl or [TBA]Br; for X = I, the solution was 0.5 M in [TBA]I.

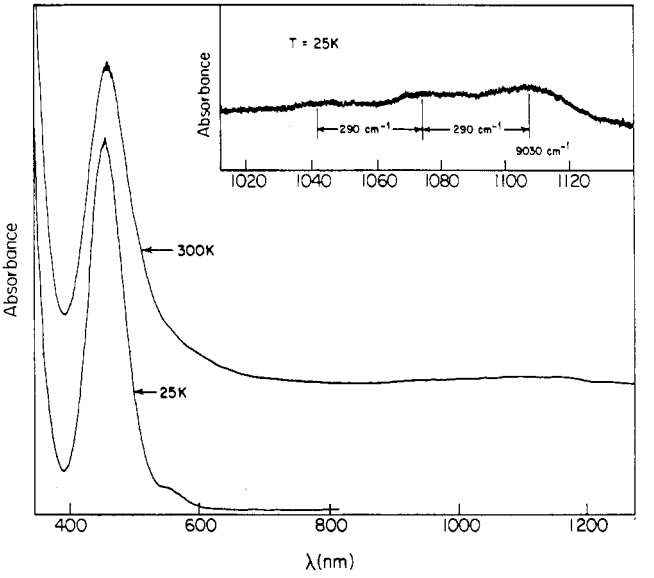

Figure 4. Absorption spectrum of $Ru_2(O_2CPr)_4Cl$ in a PMMA film cast from CH_2Cl_2 solution. The 300 K spectrum is arbitrarily shifted upward. The inset shows the lowest energy absorption at 25 K with an expanded (×10) absorbance scale.

Figure 2 shows that the visible absorption bands are only very weakly sensitive to axial ligand. Data for these and other complexes are summarized in Table I. Labels in this table are as follows: I, the weak near-infrared band previously[8] established as the $\delta \rightarrow \delta^*$ transition; II, a very poorly defined shoulder near 600 nm; III, the major visible absorption maximum; IV, UV absorption. In contrast to visible absorption, band IV is distinctly sensitive to the axial ligand. Figure 1 shows that a strong band of the monochloro complex in CH_3CN at 312 nm roughly doubles in intensity upon formation of the dichloro complex. This suggests an axial ligand-to-metal charge-transfer (LMCT) assignment.

Figure 3 confirms this assignment. The dibromo and diiodo complexes show a strong, systematic red shift of the LMCT band.[13] The general trends are very similar to those of well-established LMCT transitions in $Co^{III}L_5X$ complexes.[14]

For the diiodo complex, band III is more strongly perturbed than for the other complexes, as LMCT has dropped to nearly the same energy. This makes sense if the two transitions can mix,[15] which requires that they have the same dipole allowedness (known to be molecular *z* for III; vide infra).

Given the very long Ru–Cl bonds observed for these complexes,[9,12,16] over 0.2 Å longer than normal Ru–Cl bonds,[17] it seems unlikely that anything but a bonding–antibonding LMCT transition could be as intense as this band; observed oscillator strengths are ~0.12 for the dihalo and ~0.06 for the monohalo complexes. Figure 1 then suggests two possible assignments: $7e_u \rightarrow 6e_g$, with $\pi \rightarrow \pi^*$ character, and $7a_{1g} \rightarrow 6a_{2u}$, with $\sigma \rightarrow \sigma^*$ character. Both transitions are molecular *z* allowed. The axial ligand and metal orbitals are mixed in the σ and π molecular orbitals,[3c] which could lend intensity to the transitions. The LMCT transitions to $\delta^*(Ru_2)$ are less likely candidates for intense bands because δ^* is calculated[3c] to have no axial ligand character. Very little intensity would be expected for the transitions, and the calculated energy levels moreover suggest that such transitions would be nearly degenerate with the more strongly allowed transitions to π^*.

Intense $\sigma(X) \rightarrow \sigma^*(M_2)$ axial LMCT transitions have been observed for $[Rh_2(O_2CMe)_4X_2]^{2-}$ complexes, with similar axial ligand bond lengths,[5] at 272.5, 291, and 332 nm for, respectively, X = Cl, Br, I, all with $\epsilon \simeq 25\,000$. For those complexes there is no possibility of other types of LMCT, as metal-derived π^* and δ^* levels are filled.

That the extinction coefficients for the bands of the $Rh_2(II,II)$ complexes are much higher than those observed for the $[Ru_2(carboxylate)_4X_2]^-$ LMCT bands suggests that the latter should be assigned to $\pi(X) \rightarrow \pi^*(M_2)$ LMCT transitions, $7e_u \rightarrow 6e_g$, since π-interaction should be weaker than σ-interaction. Indeed, for $[Ru_2(O_2CPr)_4I_2]^-$ we observed a band at 307 nm (ϵ = 24 000) that could be attributed to the σ-LMCT, $7a_{1g} \rightarrow 6a_{2u}$. The

(13) The formation constants for iodide binding are extremely low, and very high concentrations of [TBA]I were needed to reach a limiting spectrum. Complexation is, however, reversible, as indicated by generation of the spectrum of the dichloro complex upon addition of [TEA]Cl to the solution.
(14) Miskowski, V. M.; Gray, H. B. *Inorg. Chem.* **1985**, *14*, 401.
(15) These two transitions are assigned in the text to $6e_u \rightarrow 6e_g$ and $7e_u \rightarrow 6e_g$, with use of the labels of Figure 1. Both transitions transform as a_{2u} (*z* dipole allowed), so coupling is possible, and they share a terminal orbital, so first-order coupling is nonzero.
(16) Bennett, M. J.; Caulton, K. G.; Cotton, F. A. *Inorg. Chem.* **1969**, *8*, 1.
(17) Hopkins, T. E.; Zalkin, A.; Templeton, D. H.; Adamson, M. G. *Inorg. Chem.* **1966**, *5*, 1427.

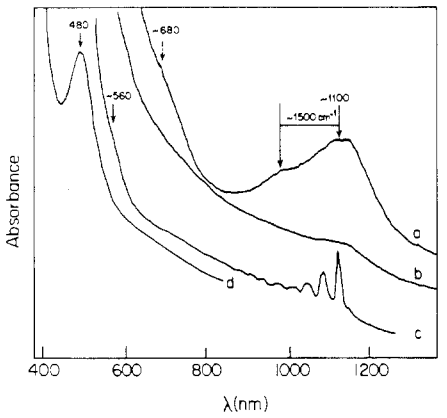

Figure 5. Absorption spectra of KBr pellets of $Ru_2(O_2CMe)_4Cl$: (a) 17 mg/365 mg of KBr, 300 K; (b) 3.8 mg/215 mg of KBr, 300 K; (c) same as in (b), but 18 K; (d) 0.4 mg/250 mg of KBr, 20 K.

Table II. Low-Temperature (15 K) Single-Crystal Absorption Spectral Data (λ_{max} (nm) with ϵ_{max} in Parentheses)

compd	$\perp Ru_2$	$\parallel Ru_2$
$Ru_2(O_2CMe)_4Cl$	560 (155), 445 (70)	~550 (140, sh)
$Ru_2(O_2CEt)_4Cl$	570 (150), 450 (95)	*b*
$Ru_2(O_2CPr)_4Cl$, 4/*m* form	572 (155), 453 (90)	~560 (150, sh)
$Ru_2(O_2CPr)_4Cl$, *I*$\bar{4}$2*d* form	548 (190), 448 (135)	570 (330)[a]
$Ru_2(O_2CPr)_4Br$, 4/*m* form	590 (150), 480 (100)	*b*

[a] $\parallel Ru_2$ spectrum, $\perp c$, is actually a 50/50 mixture of $\parallel Ru_2$ and $\perp Ru_2$ for this compound. [b] $\parallel Ru_2$ polarization not available for these compounds.

analogous transitions of Br^- and Cl^- complexes would be expected to fall at higher energy; while the strong UV absorption of these materials does blue-shift, no well-defined maxima were observed.[18]

The $7e_u \rightarrow 6e_g$ $\pi(X) \rightarrow \pi^*(M_2)$ transition was the lowest energy LMCT in Norman's calculation.[3c] Our experimental energy for the dichloro complex is higher than the calculated value by 8000 cm^{-1}, but in view of recent conclusions[19] that Xα methods can underestimate the energies of LMCT transitions, this is not surprising.

Figure 4 shows the electronic spectrum of the butyrate chloride in a poly(methyl methacrylate) (PMMA) film at room and low temperature. The room-temperature spectrum in the film is nearly identical with the solution spectrum in CH_2Cl_2 or CH_3CN, including an intense LMCT band (not shown) at 320 nm. At low temperature, band III sharpens considerably, and the poorly resolved shoulder II develops into a well-defined feature at 550 nm, while band I develops a trace of vibronic structure in an ~290-cm^{-1} progressional frequency (the excited-state $\nu(Ru_2)$), which we identify primarily by analogy to the much more sharply structured crystal spectra.[8] Representative solid-state spectra are shown in Figure 5. Inhomogeneous broadening in the polymer film is probably responsible for the broad vibronic lines.

We note that the splitting of band I by ~1500 cm^{-1}, which is observable at room temperature (Figures 2 and 5), is due to a vibronic *x,y*-polarized component of the $\delta \rightarrow \delta^*$ transition (based on an ~1450-cm^{-1} $\nu(CO_2)$ vibration)[8] rather than to two electronic excited states.[10] The only feature in the KBr pellet spectra (Figure 5) that is not also clearly evident in solution spectra is an extremely weak shoulder near 680 nm.

Single-Crystal Spectra

Our low-temperature single-crystal polarized spectra for monoclinic (*I*2/*m*) $Ru_2(O_2CMe)_4Cl$ are in good agreement with those reported by Martin et al.[9] We have obtained very similar polarized data for the σ/π face of the 4/*m* polymorph[8] of $Ru_2(O_2CPr)_4Cl$ and axial (molecular *x,y*) spectra for *I*4/*m* crystals[12] of $Ru_2(O_2CEt)_4Cl$ and 4/*m* crystals[8] of $Ru_2(O_2CPr)_4Cl$ and $Ru_2(O_2CPr)_4Br$. All of our data are summarized in Table II, where the absorptions are listed in terms of polarization relative to the Ru_2 axis.

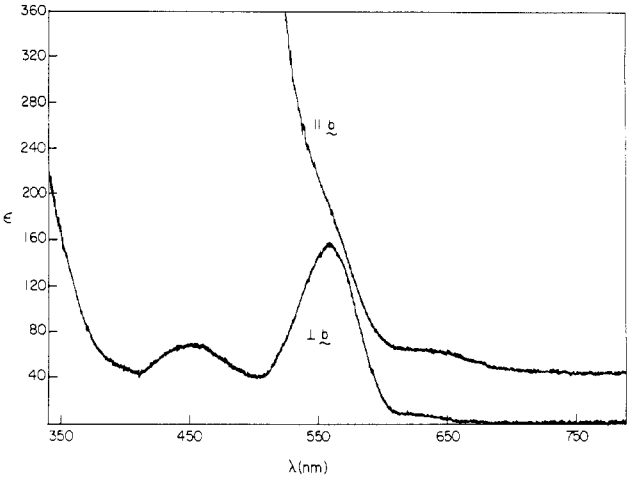

Figure 6. Absorption spectra of a single crystal of $Ru_2(O_2CMe)_4Cl$ (101 face) at 12 K. The $\parallel b$ spectrum is vertically offset by 50 ϵ units. The crystal thickness was 9 μm.

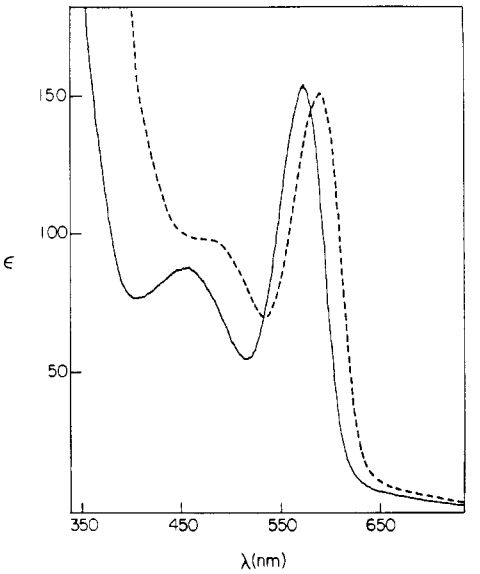

Figure 7. Axial spectra of single crystals of 4/*m* $Ru_2(O_2CPr)_4Cl$ (—) and $Ru_2(O_2CPr)_4Br$ (---) at 15 K. These are pure molecular *x,y* spectra. Crystal thicknesses were respectively 30 and 55 μm.

Spectra for $Ru_2(O_2CMe)_4Cl$ are shown in Figure 6. The $\parallel b$ and $\perp b$ spectra are $\parallel$ and $\perp$ to Ru_2, respectively.[9] Our agreement with Martin et al.[9] on the weak absorptions at 600–700 nm is significant, since they had only limited confidence in these features.

The *x,y* polarization shows two moderately intense bands at 560 and 445 nm, with a weak shoulder ($\epsilon \simeq 10$) at ~630 nm. The molecular *z*-polarized spectrum ($\parallel b$) is too intense to be measured below ~525 nm; however, weak *z*-polarized shoulders are evident near 550 and 640 nm, and it is clear that the intense ~460-nm band in the isotropic spectrum is *z*-polarized, since the $\perp z$ absorption at this wavelength is very weak.

As emphasized by Martin et al.,[9] the temperature behavior of the *x,y*-polarized absorption is characteristic of a dipole-allowed transition; the peak narrows but its intensity increases as the temperature decreases. Since the site symmetry of $Ru_2(O_2CMe)_4Cl$ is high (C_{2h}), this result strongly limits the number of possible assignments. For the less well resolved 460- and 630-nm features, the thermal behavior is inconclusive.

(18) Intense ($\epsilon \approx 20\,000$) bands that shift strongly with the reducing power of the axial halide have also been reported for the quadruply metal–metal-bonded $Re_2(O_2CR)_4X_2$ complexes. (a) Collins, D. M.; Cotton, F. A.; Gage, L. D. *Inorg. Chem.* **1979**, *18*, 1712. (b) Srinavasan, V.; Walton, R. A. *Inorg. Chem.* **1980**, *19*, 1635. No assignments are available for these features, but axial LMCT is indicated.

(19) Aizman, A.; Case, D. A. *Inorg. Chem.* **1981**, *20*, 528.

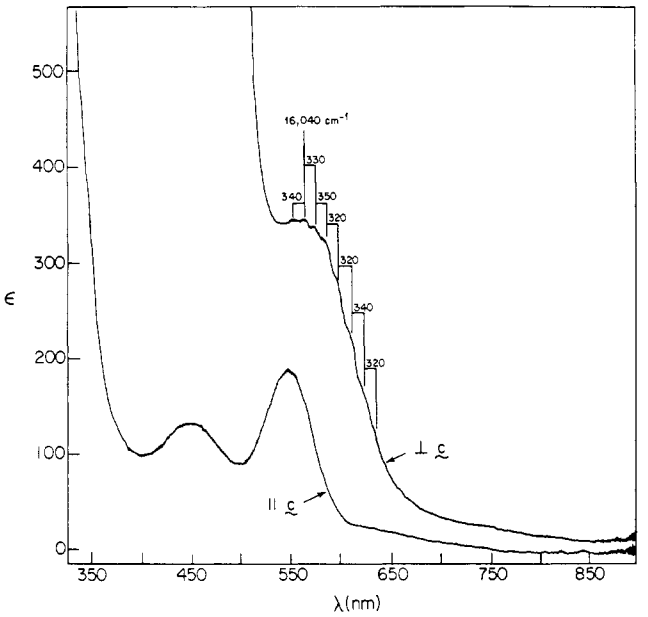

Figure 8. Single-crystal spectra of $I\bar{4}2d$ $Ru_2(O_2CPr)_4Cl$ at 8 K. The crystal was 21 μm thick. The $\perp c$ spectrum is vertically offset from $\| c$ by 15 ϵ units.

Figure 7 shows axial (molecular x,y) spectra for the $4/m$ polymorphs[8] of $Ru_2(O_2CPr)_4Cl$ and $Ru_2(O_2CPr)_4Br$. The very marked color difference of the axial faces for chloride (blue-gray) and bromide (green) proves to be largely due to a red shift of intense high-energy absorption. Neither dominant x,y-polarized absorption is strongly shifted by halide, as judged by comparison to authentic LMCT transitions discussed earlier; we therefore feel that none of these weak bands can be assigned to axial LMCT transitions.[20]

Figure 8 shows polarized single-crystal spectra for the $I\bar{4}2d$ polymorph[16] of $Ru_2(O_2CPr)_4Cl$. In the oriented gas approximation,[8] the $\| c$ spectrum of this lattice is a pure $\perp z$ spectrum, while the $\perp c$ spectrum is a 50:50 mixture of $\perp z$ and $\| z$. The $\| c$ spectrum agrees with other $\perp z$ spectra, although it is somewhat more intense, perhaps as a result of the low symmetry. The $\perp c$ spectrum is clearly anomalous.

There is a rather intense ($\epsilon \simeq 330$) $\perp c$-polarized shoulder maximizing near 570 nm. It shows the only vibronic structure we have identified in any of our visible spectra: a long progression in an $\sim$330-cm^{-1} vibrational interval. In view of the poor definition of the structure, we should emphasize that it was reproducibly observed for three different crystals with thicknesses varying by a factor of 2, so optical artifacts have been eliminated as an explanation of it.

This frequency interval is in perfect agreement with the ground-state $\nu(Ru_2)$ totally symmetric stretching frequency.[8,21] However, the fact that the progression is so long (large Franck–Condon factor) implies a large bond-distance change along the involved normal coordinate. For metal–metal $\delta \rightarrow \delta^*$ transitions, I_{10}/I_{00} intensity ratios on the order of 1 generally[6-8] correspond to excited-state reduction of $\nu(M_2)$ by $\sim$10%. The far higher Franck–Condon factor observed here is totally inconsistent with an unchanged $\nu(Ru_2)$ being the Franck–Condon active vibrational mode.

We suggest that the a_{1g} ν(Ru–O) mode is a better candidate. The ground-state value is[22] 440 cm^{-1}, so a large reduction in excited-state stretching frequency would be implied. And such large geometry changes along the Ru–O coordinate strongly suggest that the electronic transition involves population of the σ^*(Ru–O) orbitals, $5b_{1g}$ and $4b_{2u}$ of Figure 1. The long progression is similar to that observed for mononuclear complexes[23] in ligand field transitions that involve population of $d\sigma^*$(M–L) orbitals.

The lowest energy candidates for such a transition are π^* and/or $\delta^* \rightarrow \sigma^*$(Ru–O) (Figure 1). Why should such a transition have become so intense for $I\bar{4}2d$ $Ru_2(O_2CPr)_4Cl$? We think the answer is that the $I\bar{4}2d$ lattice yields[16] a low ($C_2 \perp$ to Ru_2) site symmetry for the Ru_2 chromophore and that, because the $(Ru_2Cl)_\infty$ chains are nonlinear, the symmetry lowering is electronically significant. We observed other manifestations of symmetry lowering in the near-infrared spectra that were reported in our previous paper.[8]

Both $\pi^*(Ru_2)$ and $\delta^*(Ru_2) \rightarrow \sigma^*$(Ru–O) become formally allowed $\perp c$ in the C_2 site symmetry. Since a strong molecular z-polarized ($\perp c$ in this lattice) transition exists just to higher energy, there is a mechanism available for intensity stealing in the low-symmetry site.

The calculations of Norman et al.[3c] indicate that π^* and δ^* are nearly degenerate, so transitions from the two orbitals to σ^*(Ru–O) should be roughly the same energy. The $\pi^* \rightarrow \sigma^*$(Ru–O) transition is allowed even in D_{4h}, but x,y, via the $5e_g \rightarrow 4b_{2u}$ component. We assign the $\sim$560-nm x,y-polarized band (Table II) of all of the compounds to this transition, and the z-polarized shoulder (at about the same wavelength) can be assigned to δ^* and/or $\pi^* \rightarrow \sigma^*$(Ru–O). Both transitions are dipole-forbidden in z polarization in D_{4h} symmetry; both could acquire vibronic or low-symmetry-induced z-polarized intensity.

We suspect that the vibronic structure of the $\perp c$ absorption of $I\bar{4}2d$ $Ru_2(O_2CPr)_4Cl$ should be assigned to the $\delta^* \rightarrow \sigma^*$(Ru–O) transition. The δ-symmetry metal orbitals are less strongly metal–metal bonding than the π-symmetry metal orbitals,[3] so $\delta^* \rightarrow \sigma^*$(Ru–O) should have smaller $\nu(Ru_2)$ Franck–Condon factors than $\pi^* \rightarrow \sigma^*$(Ru–O). Simultaneous vibronic excitation of $\nu(Ru_2)$ and ν(Ru–O) might account for the absence of resolved vibronic structure in the x,y-polarized absorption, assigned to $\pi^* \rightarrow \sigma^*$(Ru–O). For $\delta^* \rightarrow \sigma^*$(Ru–O), we expect the $\nu(Ru_2)$ I_{10}/I_{00} values to be as small or smaller than those found[8] for $\delta \rightarrow \delta^*$, which are about 0.6. It is likely, then, that weak progressions involving $\nu(Ru_2)$ are responsible in part for the low resolution of the ν(Ru–O) vibronic structure.

These assignments tie in with our recent interpretation[5] of the electronic spectra of $Rh_2(O_2CMe)_4L_2$ compounds. The $\pi^*(Rh_2) \rightarrow \sigma^*$(Rh–O) transition of these molecules, structured[4,5] in ν(Rh–O) $\simeq$ 300 cm^{-1} in the case of the aquo complex, was assigned at $\sim$600 nm, with $\delta^*(Rh_2) \rightarrow \sigma^*$(Rh–O) observed as a z-polarized transition at slightly longer wavelength. Norman's calculations[3c] predict that these transitions should be blue-shifted for the diruthenium(II,III) compounds, in agreement with observation, but predictions of the transition energies, as previously noted,[5] are a bit high. The calculations do, however, support the idea that transitions of the ruthenium carboxylates analogous to those of the rhodium(II) carboxylates should occur at similar energies. Earlier we suggested[5] reasons transitions such as $\pi^*(M_2) \rightarrow \sigma^*(M_2)$ are at much higher energy than transitions to σ^*(M–O).

We think that the $\sim$450-nm x,y-polarized band is simply the intense z-polarized band that appears at this wavelength in isotropic spectra, appearing weakly in x,y polarization as a result of vibronic or low-symmetry perturbation. The fact that the shift to longer wavelength of this band upon replacement of Cl^- by Br^- (Figure 7, Table II) is about the same as the shift of the intense solution band (Figure 3, Table I) is persuasive in this regard.

For the weak $\sim$630-nm absorption, our data are not very informative. One candidate for this assignment should be mentioned, the $\delta \rightarrow \pi^*$ excitation, $2b_{2g} \rightarrow 6e_g$ of Figure 1. As a LaPorte-forbidden transition, it should be weak; intensity in both

(20) This conclusion is weakest for the $\sim$630-nm shoulder, which is not well-resolved in the spectra.
(21) Clark, R. J. H.; Ferris, L. T. H. *J. Am. Chem. Soc.* **1981**, *20*, 2759.
(22) This value is from our work;[8] Clark and Ferris[21] assigned this mode at 380 cm^{-1}. For present purposes, the distinction between the two assignments is unimportant. Either one yields a large reduction in excited-state frequency. The vibrational force field for these molecules seems to be a rather complex one,[8] so calculations of excited-state geometry changes are not straightforward.
(23) (a) Yersin, H.; Otto, H.; Zink, J. I.; Gliemann, G. *J. Am. Chem. Soc.* **1980**, *102*, 951. (b) Wilson, R. B.; Solomon, E. I. *J. Am. Chem. Soc.* **1980**, *102*, 4085.

polarizations would be vibronically induced. While an MO diagram (Figure 1) places it at about the same energy[3c] as $\delta \rightarrow \delta^*$, proper account of electron repulsion[24] could lead to a shift to higher energy of the required magnitude. The ~630-nm band is the lowest energy candidate for $\delta \rightarrow \pi^*$ according to our near-infrared results.[8] Excitations such as $\pi \rightarrow \delta^*$ are also plausible candidates but would be expected[6b] at higher energy.

We finally consider the intense *z*-polarized absorption, $\lambda_{max} \simeq$ 460 nm. Norman et al.[3c] have assigned this transition to $6e_u \rightarrow 6e_g$ (Figure 1). Since no vibronic structure was observed for this band, we can only note that the observed $\|z$ polarization is consistent with this assignment. One puzzling feature is that resonance Raman spectra for excitation into this band show patterns of ground-state vibrational intensification[21] that are similar to the vibronic intensity pattern seen for the $\delta \rightarrow \delta^*$ transition[8] and also to Raman spectra observed for $\delta \rightarrow \delta^*$ excitation of other compounds;[6a] namely, long progressions in $\nu(M_2)$ are observed. The $\delta \rightarrow \delta^*$ excitation is calculated[3c] to be a rather pure metal–metal transition, whereas interaction between metal–metal and carboxylate orbitals of e_u symmetry results in the calculated $6e_u$ orbital having a great deal of carboxylate character. So $6e_u \rightarrow 6e_g$ is expected to have LMCT character, according to the calculation, whereas the resonance Raman data suggest a pure metal–metal $\pi \rightarrow \pi^*$ transition. There is not, however, necessarily any contradiction here, as relaxation effects might result in the excitation being more metal–metal-localized than ground-state orbitals suggest. In any case, this is the lowest energy excitation of the $\pi \rightarrow \pi^*$ type.

Intensities of Metal–Metal Transitions

From the data for monochloro and dichloro $Ru_2(O_2CPr)_4^+$ complexes (Table I), we estimate oscillator strengths for the $\delta \rightarrow \delta^*$ transition of 0.0006 and 0.0009, respectively. The intensity of the transition increases as the energy of axial LMCT decreases (Table I), which we attribute to a small degree of mixing between these two molecular *z*-polarized transitions.

The oscillator strength of the ~23 000-cm^{-1} band of $Mo_2(O_2CH)_4$ that is now[7] assigned as $\delta \rightarrow \delta^*$ has been estimated[3a] to be 0.0008. Thus, the intensity of $\delta \rightarrow \delta^*$ is not very sensitive to metal–metal bond length and/or bond order for these carboxylate-bridged complexes. The large shift in $\delta \rightarrow \delta^*$ energy between the Mo_2 and Ru_2 complexes is not predominantly a one-electron effect, but instead results from differences in electron repulsion contributions[6,24,25] to the transition energy for $\delta^2(\delta^*)^0$ and $\delta^2(\delta^*)^1$ ground-state configurations; the two-electron terms roughly cancel out for $\delta^2(\delta^*)^1$.

The low oscillator strengths[26] and $\nu(M_2)$ Franck–Condon factors indicate[27] that the δ-symmetry metal–metal interaction must be very weak, and as discussed in detail elsewhere,[3,25] much of the δ/δ^* splitting is attributable to interaction of carboxylate orbitals with the δ/δ^* orbitals, rather than to direct metal–metal interaction.

We finally note that the only other well-established example of a metal–metal $\pi \rightarrow \pi^*$ transition is that of $Re_2X_8^{2-}$; it is assigned to an intense ($f \simeq 0.2$) band at 38 000 cm^{-1}. That its intensity is so much greater than that of the lowest $\pi \rightarrow \pi^*$ transition of the ruthenium carboxylates (~22 000 cm^{-1}, $f \simeq 0.02$) presumably reflects some combination of mixing with halide-to-metal CT transitions (analogous to that required[25] to explain the relatively high intensity of the $\delta \rightarrow \delta^*$ transition of $Re_2Cl_8^{2-}$), stronger metal–metal π-bonding, and differing metal–metal character in the electronic transition.

Acknowledgment. We thank Don Martin and Steve Rice for helpful discussions. This research was supported by National Science Foundation Grant CHE84-19828.

Registry No. PMMA, 9011-14-7; $[Ru_2(O_2CH)_4Cl_2]^-$, 71767-76-5; $Ru_2(O_2CPr)_4Cl$, 47511-63-7; $[Ru_2(O_2CPr)_4Cl_2]^-$, 114595-61-8; $[Ru_2(O_2CPr)_4Br_2]^-$, 114595-62-9; $[Ru_2(O_2CPr)_4I_2]^-$, 114595-63-0; $Ru_2(O_2CMe)_4Cl$, 38833-34-0; $Ru_2(O_2CEt)_4Cl$, 71061-91-1; $Ru_2(O_2CPr)_4Br$, 107053-30-5; $Ru_2(O_2CPr)_4^+$, 114691-50-8.

(24) Noodleman, L.; Norman, J. G., Jr. *J. Chem. Phys.* **1979**, *70*, 4903.
(25) Hopkins, M. D.; Gray, H. B.; Miskowski, V. M. *Polyhedron* **1987**, *6*, 705.
(26) The $\delta \rightarrow \delta^*$ oscillator strengths listed here include[7,8] contributions from vibronically induced *x,y* components, so the oscillator strengths for the molecular *z*-dipole-allowed transitions are even lower.
(27) Mulliken, R. S. *J. Chem. Phys.* **1939**, *7*, 20.
(28) Mortola, A. P.; Moskowitz, J. W.; Rosch, N.; Cowman, C. D.; Gray, H. B. *Chem. Phys. Lett.* **1975**, *32*, 283.

Contribution from the Chemistry Department, University of Tasmania, Box 252C, Hobart, Tasmania, Australia, and Institut für Anorganische Chemie der Justus-Liebig-Universität, Heinrich-Buff Ring 58, 6300 Giessen, FRG

Electronic and Raman Spectra of the Linear NiO_2^{2-} Ion in K_2NiO_2

Michael A. Hitchman,*,† Horst Stratemeier,† and Rudolf Hoppe*,‡

Received October 30, 1987

The polarized spectrum of a single crystal of K_2NiO_2 is reported over the range 3000–22 500 cm^{-1} and assigned on the basis of a ligand field calculation. The d-orbital energies imply significant configuration interaction between the metal $3d_{z^2}$ and 4s orbitals in the linear NiO_2^{2-} ion. Vibrational fine structure in the optical spectrum suggests that in the $^3\pi_g$ excited state the energy of the totally symmetric stretching vibration decreases significantly from the ground-state value observed in the Raman spectrum, and this is correlated with the expected increase in the equilibrium Ni–O bond length. The extreme dichroism of the band in the visible region may be explained by considering the nature of the two electronic states involved in the transition and the form of the intensity-inducing vibrations.

Introduction

The electronic spectra of numerous tetragonally distorted nickel(II) complexes have been reported,[1] and these have frequently been used to test models of the bonding in transition-metal compounds.[2] However, such compounds have usually involved a tetragonal weakening of the ligand field, with the extreme limit of this kind of distortion producing a square-planar geometry. These planar metal complexes are unusual because it is impossible to explain their energy levels satisfactorily without including the higher energy metal s orbital in the bonding scheme.[3,4] Just as

* To whom correspondence should be addressed: M.A.H., spectroscopic aspects; R.H., structural and preparative aspects.
† University of Tasmania.
‡ Institut für Anorganische Chemie der Justus-Liebig-Universität.

(1) For a comprehensive listing of the spectra of tetragonal nickel(II) complexes see: Lever, A. B. P. *Inorganic Electronic Spectroscopy*, 2nd ed.; Elsevier: Amsterdam, 1984; Chapter 6.
(2) See ref 1, Chapter 9.
(3) Hitchman, M. A.; Bremner, J. B. *Inorg. Chim. Acta* **1978**, *27*, L61–L63. Vanquickenborne, L. G.; Ceulemans, A. *Inorg. Chem.* **1981**, *20*, 796. Deeth, R. J.; Hitchman, M. A. *Inorg. Chem.* **1986**, *25*, 1225.

0020-1669/88/1327-2506$01.50/0